

Enhancing CO₂ electrolysis performance with various metal additives (Ru, Co, Fe, and Ni) - decorated La(Sr)Fe(Mn)O₃ cathode in solid oxide electrolysis cells

Sang Won Lee^{a, b}, *Tae Heon Nam*^{a, c}, *Min Kyu Kim*^a, *Seokhee Lee*^a, *Kyu Hyung Lee*^{*c}, *Jong Hyeok Park*^{*b}, and *Tae Ho Shin*^{*a}

^a Korea Institute of Ceramic Engineering and Technology, Jinju-si, Gyeongsangnam-do 52851, Republic of Korea.

^bDepartment of Chemical and Biomolecular Engineering, Yonsei University, 50 Yonsei-ro, Seodaemun-gu, Seoul, 120-749, Republic of Korea.

^c Department of Materials Science & Engineering, Yonsei University, 50 Yonsei-ro, Seodaemun-gu, Seoul, 120-749, Republic of Korea.

Supporting Information Table of Contents:

Figure S1 (a) Cross-sectional SEM image of LSGM supported cell with LSFM electrode (b) SEM image of pristine LSFM electrode with high magnification.

Figure S2. CO₂ electrolysis performance of the cell using an LSFM electrode with different metal additives feeding 50% CO₂ - 50% CO at various temperatures; (a) LSFM, (b) LSFM-Ru, (c) LSFM-Co, (d) LSFM-Fe, and (e) LSFM-Ni

Figure S3. Impedance spectra of the LSFM electrode with and without different metal additives at various temperatures under 50% CO₂ - 50% CO; (a) LSFM, (b) LSFM-Ru, (c) LSFM-Co, (d) LSFM-Fe, and (e) LSFM-Ni.

Figure S4. DRT plot from the EIS of the LSFM electrode with and without different metal additives at various temperatures under 50% CO₂ - 50% CO; (a) LSFM, (b) LSFM-Ru, (c) LSFM-Co, (d) LSFM-Fe, and (e) LSFM-Ni.

Figure S5 SEM images of metal-infiltrated LSFM electrode after cell test for CO₂ Reduction; (a) LSFM-Ru, (b) LSFM-Co, (c) LSFM-Fe, and (d) LSFM-Ni.

SUPPORTING INFORMATION

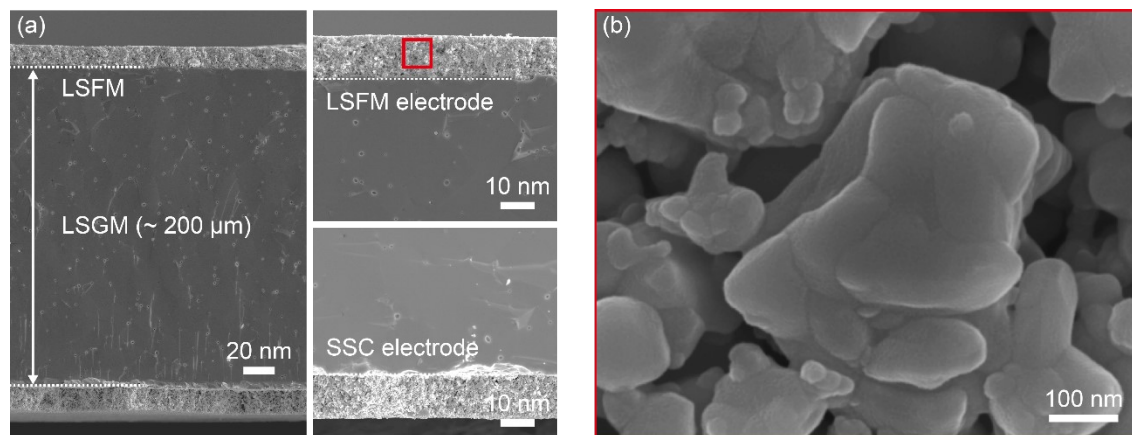


Figure S1 (a) Cross-sectional SEM image of LSGM supported cell with LFSM electrode (b) SEM image of pristine LFSM electrode with high magnification.

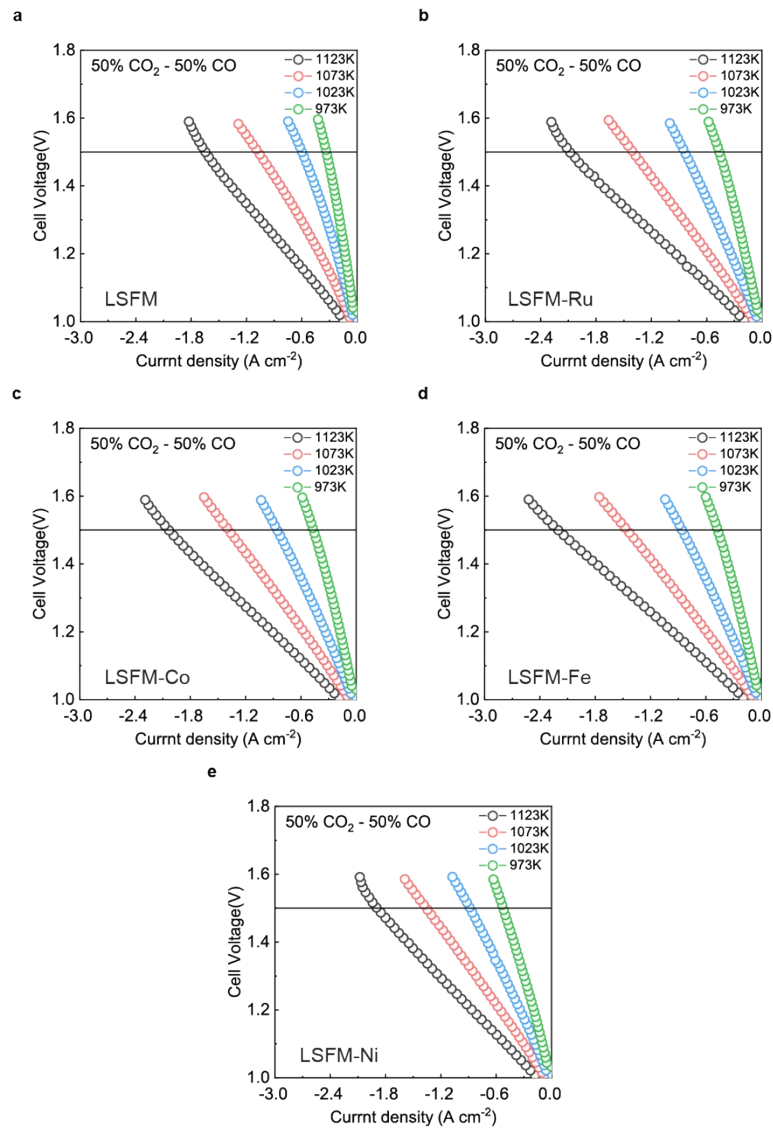


Figure S2. CO₂ electrolysis performance of the cell using an LSFM electrode with different metal additives feeding 50% CO₂ - 50% CO at various temperatures; (a) LSFM, (b) LSFM-Ru, (c) LSFM-Co, (d) LSFM-Fe, and (e) LSFM-Ni.

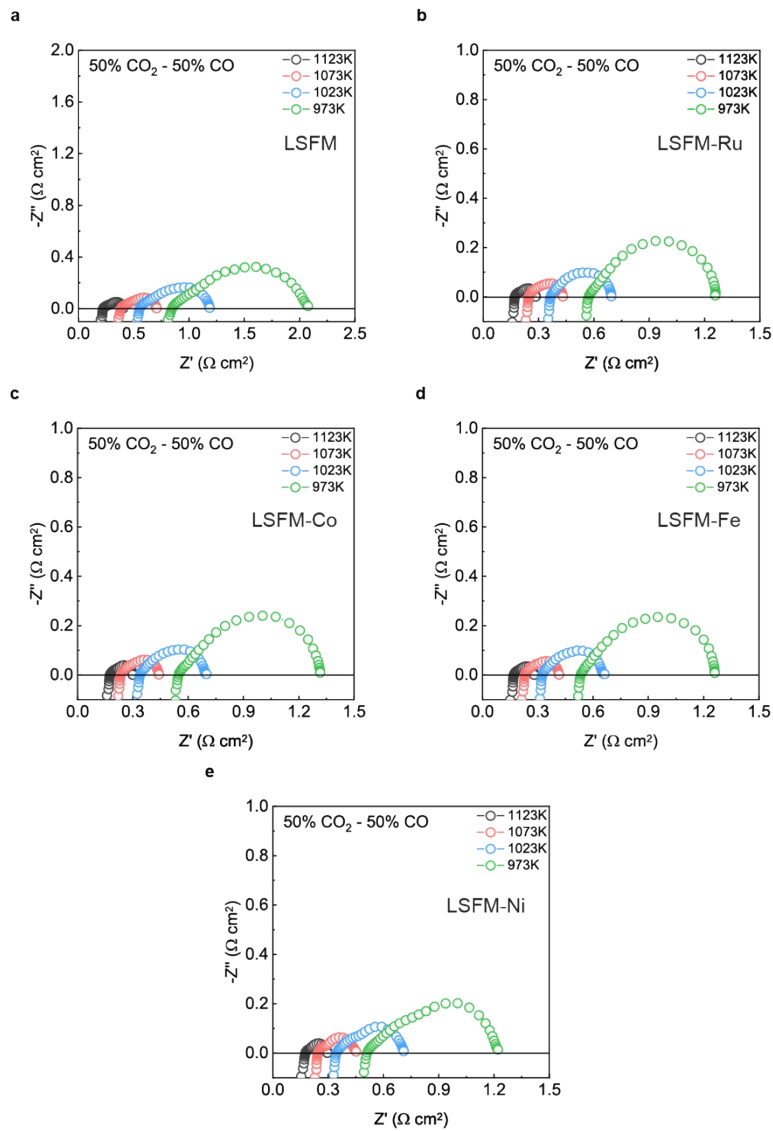


Figure S3. Impedance spectra of the LSFM electrode with and without different metal additives at various temperatures under 50% CO₂ - 50% CO; (a) LSFM, (b) LSFM-Ru, (c) LSFM-Co, (d) LSFM-Fe, and (e) LSFM-Ni.

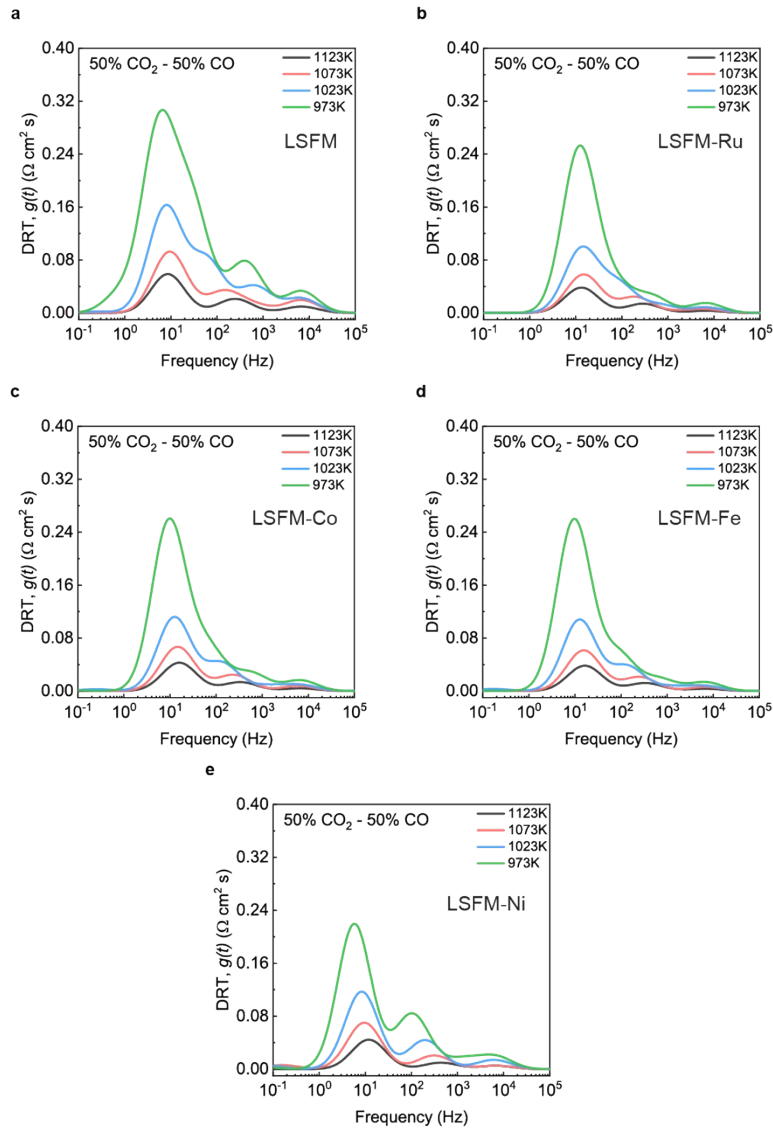


Figure S4. DRT plot from the EIS of the LSFM electrode with and without different metal additives at various temperatures under 50% CO_2 - 50% CO; (a) LSFM, (b) LSFM-Ru, (c) LSFM-Co, (d) LSFM-Fe, and (e) LSFM-Ni.

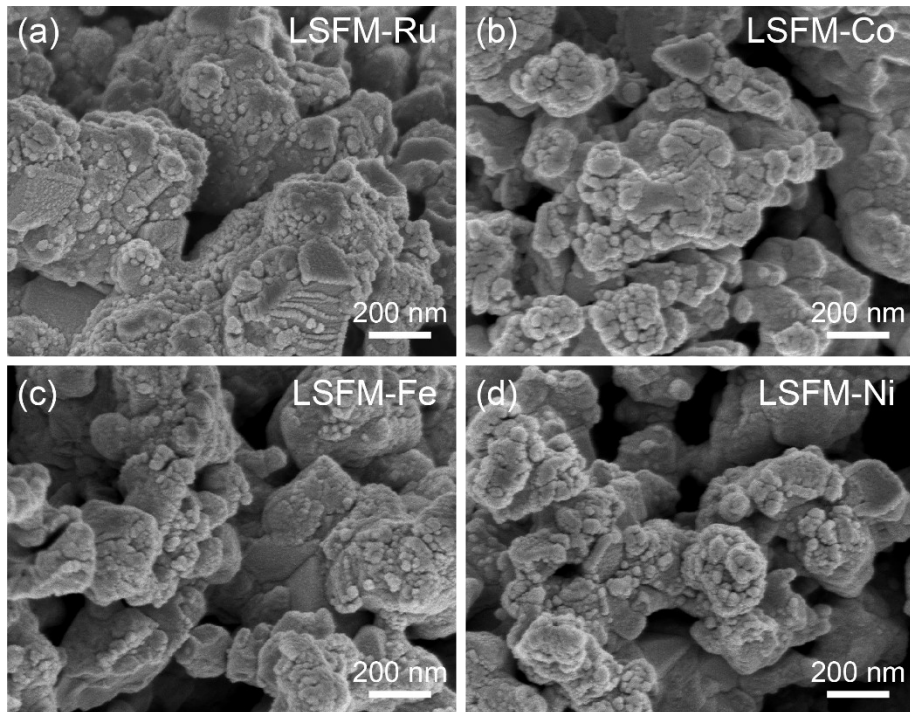


Figure S5 SEM images of metal-infiltrated LSFM electrode after cell test for CO₂ Reduction; (a) LSFM-Ru, (b) LSFM-Co, (c) LSFM-Fe, and (d) LSFM-Ni.